Computational Visual Media
DOI 10.1007/s41095-015-0004-6 Vol. 1, No. 1, March 2015, 27–35

Research Article

Least-squares images for edge-preserving smoothing

Hui Wang[1], Junjie Cao[2], Xiuping Liu[2] (✉), Jianmin Wang[1], Tongrang Fan[1], and Jianping Hu[3]

Abstract In this paper, we propose least-squares images (LS-images) as a basis for a novel edge-preserving image smoothing method. The LS-image requires the value of each pixel to be a convex linear combination of its neighbors, i.e., to have zero Laplacian, and to approximate the original image in a least-squares sense. The edge-preserving property inherits from the edge-aware weights for constructing the linear combination. Experimental results demonstrate that the proposed method achieves high quality results compared to previous state-of-the-art works. We also show diverse applications of LS-images, such as detail manipulation, edge enhancement, and clip-art JPEG artifact removal.

Keywords feature-preserving; image enhancement; image smoothing; least-squares images (LS-images)

1 Introduction

Edge-preserving image smoothing has emerged as a valuable tool for many applications in image processing and computer graphics, and has received much attention [1–12]. However, it is still a challenging problem due to the difficulty of distinguishing sharp edges from noises.

Of the previous methods for edge-preserving image smoothing, some are gradient domain methods, which generally specify both zeroth-order constraints to provide desired pixel values and first-order differential constraints to provide desired pixel gradients, examples being the total variation model [2], WLS optimization [5], and L_0 smoothing [9, 12]. Inspired by use of second-order differential Laplacian constraints for image colorization [13] and segmentation [14], we propose least-squares images (LS-images) as a basis for a novel edge-preserving image smoothing method. The LS-image is constructed with inhomogeneous Laplacian constraints set to zero and approximates the original image in a least-squares sense. The edge-preserving property is achieved by using edge-aware weights to compute the inhomogeneous Laplacian. Minimizing second-order Laplacians with vertex constraints has been widely used in digital geometry processing, for purposes such as smoothing [15, 16], geometry compression [17], and high-pass quantization [18].

Experimental results demonstrate the proposed method achieves high quality results. The LS-image is simple, robust, and versatile, and may be used in many of the applications that have so far been based on previous approaches. It can be used for detail manipulation, edge enhancement, and clip-art compression artifact removal.

The rest of this paper is organized as follows. Section 2 describes previous work on edge-preserving image smoothing. The LS-image is introduced in Section 3. Experimental results and comparisons with existing methods are discussed in Section 4. Applications of LS-images are demonstrated in Section 5. Finally this paper is concluded in Section 6.

2 Previous work

Edge-preserving image smoothing, which smooths small details and preserves sharp edges, has already received a great deal of attention. A full review

1 School of Information Science and Technology, Shijiazhuang Tiedao University, Shijiazhuang 050043, China.
2 School of Mathematical Sciences, Dalian University of Technology, Dalian 116024, China. E-mail: xpliu@dlut.edu.cn (✉).
3 School of Sciences, Northeast Dianli University, Jilin 132012, China.

Manuscript received: 2014-09-26; accepted: 2015-01-19

of edge-preserving image smoothing is beyond the scope of this paper. In this section, only approaches that are most relevant to the proposed one are surveyed.

2.1 Explicit weighted-average methods

Classical bilateral filtering [3] is perhaps the simplest and most intuitive of the explicit weighted-average methods. It smooths each pixel as a linear combination of its neighbors, where weights consider both spatial distance and range similarity. A number of efficient implementations of bilateral filtering have been proposed [19–21]. A bilateral texture filter has also been proposed to effectively remove textures while preserving structures [22]. Mean shift filtering [4] can also be regarded as an explicit weighted-average method, where a moving window is used to compute the average. Edge-avoiding wavelets with explicit image-adaptive weights can also be used for edge-preserving image smoothing [7]. However, constraints on kernel size of the wavelet may limit its applicability. Derived from a local linear model between a guidance image and the final filtering result, explicit and efficient guided filtering has been used for edge-preserving image smoothing [11]. Another class of explicit edge-preserving filtering uses weights based on geodesic distances between pixels [23, 24]. Karacan et al. [25] proposed an explicit structure-preserving image smoothing method, where the weights are derived from region covariances. Learning an image filter from a pair of example images is considered in Ref. [26].

As stated in Ref. [11], the local explicit weighted-average methods have one limitation: unavoidable halos appear near certain weak edges. Global implicit methods attenuate these halos, at the price of high computational cost. Our proposed edge-preserving image smoothing method is a global implicit approach.

2.2 Gradient based methods

As a first-order differential quantity, the gradient contains information about details, and has been widely used in edge-preserving image smoothing [1, 5, 9, 12]. Anisotropic diffusion achieves edge-preserving smoothing by use of an edge-stopping function to permit smoothing only in the interior of regions without crossing sharp edges; the edge-stopping function is based on magnitudes of the gradients [1]. The flexible weighted least-squares optimization framework achieves edge-preserving smoothing by minimizing gradients using edge-aware weights [5]. Reconstructing images that minimize gradients in the L_0 norm is another state-of-the-art edge-preserving smoothing approach [9, 12]. Xu et al. [27] proposed a new inherent variation and relative total variation measures, and developed an efficient optimization system to extract main structures from textures.

In this paper, the LS-image approach minimizes the Laplacian, which is a second-order differential quantity, to provide smoothing. The edge-preserving property of the LS-image is inherited from the edge-aware inhomogeneous Laplacian.

2.3 Other approaches

Paris et al. [10] manipulated the coefficients of the Laplacian pyramid around each pixel to provide edge-preserving smoothing. A mixed-domain edge-aware image manipulation method based on Gaussian pyramids was given in Ref. [28]. Inspired by the 1D Hilbert–Huang transform (HHT), Subr et al. [6] proposed an edge-preserving image smoothing method based on averaging two envelops which fit the local maxima and minima of the image. An efficient structure-aware image smoothing method based local extrema on space-filling curves was proposed in Ref. [29]. Edge-aware image smoothing methods have also been used for image and video abstraction [30, 31].

3 Edge-preserving smoothing via LS-image

In this section, we first describe a novel edge-preserving smoothing method via the proposed LS-image, and then analyse the mathematical relationship of our method to other related work.

3.1 LS-image

Given an original image $\boldsymbol{g}$ (gray or color) with n pixels, the LS-image $\boldsymbol{u}$ is an edge-preserving smoothing result, which minimizes the following energy:

$$\sum_{i=1}^{n}\left(\lambda\|\boldsymbol{u}(i)-\boldsymbol{g}(i)\|^2+\|\boldsymbol{u}(i)-\sum_{j\in N(i)} w_{ij}\boldsymbol{u}(j)\|^2\right) \quad (1)$$

where i denotes the index of a pixel. The data term $\|\boldsymbol{u}(i) - \boldsymbol{g}(i)\|^2$ ensures the LS-image approximates the original image, while the smoothing term constrains the value of each pixel to be a convex combination of the values of its neighbors $N(i)$, so that each pixel has a zero Laplacian. As explained in Section 4.2, in this paper we fix $N(i)$ to be the 3×3 neighborhood of pixel i. The parameter λ allows a trade-off between the data and smoothing terms; decreasing λ leads to a smoother LS-image $\boldsymbol{u}$.

The non-linear weights w_{ij} play an important role in the edge-preserving properties of LS-images. They are set as follows:

$$w_{ij} \propto \exp(-\beta\|\boldsymbol{g}(i) - \boldsymbol{g}(j)\|^2) \tag{2}$$

where $\sum_{j\in N(i)} w_{ij} = 1.0$, and β is a parameter to control the edge-preserving extent; increasing β preserves more features. Gaussian weights as above have been widely used, for image colorization [13], image segmentation [14], and computation of envelopes from extrema [6]. As noted for image segmentation [14], it is useful to normalize the squared distances $\|\boldsymbol{g}(i) - \boldsymbol{g}(j)\|^2,\ \forall j \in N(i)$, $i = 1, \cdots, n$, before computing the weights.

The energy in Eq. (1) can be uniquely minimized as the solution of the following linear system:

$$(\lambda\boldsymbol{I} + \boldsymbol{L}^{\mathrm{T}}\boldsymbol{L})\boldsymbol{u} = \lambda\boldsymbol{g} \tag{3}$$

where $\boldsymbol{I}$ is the n-dimensional identity matrix, and $\boldsymbol{L}$ is an $n \times n$ inhomogeneous Laplacian matrix with elements

$$L_{ij} = \begin{cases} 1, & i = j \\ -w_{ij}, & j \in N(i) \\ 0, & \text{otherwise} \end{cases} \tag{4}$$

3.2 Relation to other work

Bilateral filter. As stated in Eq. (3), our edge-preserving LS-image may be expressed as applying the operator $\mathbf{LS}_{\lambda,\beta} = \lambda(\lambda\boldsymbol{I} + \boldsymbol{L}^{\mathrm{T}}\boldsymbol{L})^{-1}$ to the original image vector $\boldsymbol{g}$. Each row of $\mathbf{LS}_{\lambda,\beta}$ could be thought as a kernel that determines the value of the corresponding pixel as a weighted combination of other pixels in the original image.

In Fig. 1, we compare our filter kernels with classical bilateral filters in Ref. [3]. Firstly, it can be seen that filter kernels of the both two methods are edge-aware, and thus our smoothing method is spatially-variant filtering. Secondly, the support of filter kernels of our LS-image is much larger than the 3×3 neighbors in Eq. (1).

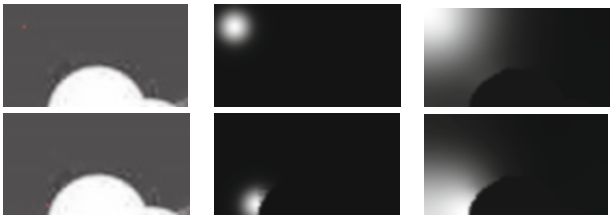

(a) Input image (b) Bilateral filter (c) Our LS-image

Fig. 1 Filter kernels. Left: kernels are centered at the pixels denoted by the red dots. Middle: filter kernels for bilateral filtering with $\delta_s = 5$ and $\delta_r = 0.1$. Right: filter kernels for LS-images with $\beta = 100$ and $\lambda = 10^{-5}$.

Weighted least-squares method. Both the LS-image and weighted least-squares (WLS) method in Ref. [5] can preserve sharp edges, by solving a linear system. The linear system for WLS is

$$(\boldsymbol{I} + \lambda\boldsymbol{L}_g)\boldsymbol{u} = \boldsymbol{g} \tag{5}$$

where $\boldsymbol{L}_g$ is a five-point spatially inhomogeneous Laplacian matrix, while the matrix $\boldsymbol{L}$ in Eq. (3) is an extended ten-point spatially inhomogeneous Laplacian matrix.

The smoothness term in WLS minimizes a first-order differential quantity, gradient, while the LS-image approach minimizes a second-order differential quantity, the Laplacian. The edge-preserving property of WLS is achieved by minimizing homogeneous gradients with edge-aware weights, while LS-image uses edge-aware weights for computing the inhomogeneous Laplacian. In geometry processing, minimizing the Laplacian corresponds to plate energy, while minimizing gradients corresponds to membrane energy [32].

We compare our LS-image with the WLS method in Fig. 2, which demonstrates that our approach can generate clearer edges—see particularly the two cars in the top region. This is because WLS only considers the 4 nearest neighbors of a pixel in Eq. (5), while our LS-image approach takes into account the 25 nearest neighbors in Eq. (3). Thus, the interaction range τ, defined in Section 5 in Ref. [8], is $\tau = 1$ for WLS, while $\tau = 2$ for LS-images.

Image segmentation and colorization. The edge-aware smoothing term of our LS-image approach in Eq. (1) is inspired by a colorization method based on optimization [13], and random walks for segmentation [14]. However, these works use sparse and hard constraints, while in LS-images, all pixels are constrained in a soft linear squares sense for edge-preserving image smoothing.

(a) Input image (b) WLS ($\lambda = 0.2, \alpha = 1.2$) (c) Ours ($\beta = 1500, \lambda = 10^{-4}$)

Fig. 2 Comparing our LS-image with the WLS result [5].

4 Implementation and results

In this section, we discuss implementation details, demonstrate that our method producing artifact-free results, and compare it to previous state-of-the-art approaches.

4.1 Implementation

Our algorithms were implemented in MATLAB on a PC with a 3.30 GHz Intel (R) core (TM) i3 CPU and 3.20 GB of RAM. They were not optimized for speed. The most time-consuming part of our method is solving the linear system in Eq. (3), using the built-in solver of MATLAB. It takes about 2 s for the 384 × 512 image in Fig. 3. A C++ implementation on a GPU would speed up our method.

4.2 Parameters

The LS-image approach has three parameters: choice of neighborhood $N(i)$, λ to trade off smoothing and edge-preservation, and β for computing weights.

Figure 4 demonstrates the effects of choosing different neighborhoods $N(i)$. It can be seen that enlarging $N(i)$ gives better results, as observed in Ref. [8]. However, a larger $N(i)$ would destroy the sparse property of the inhomogeneous Laplacian matrix, and induce expensive computational cost. In this paper, we fixed $N(i)$ to be the 3×3 neighbors of pixel i, following Refs. [6, 13].

In Fig. 3, LS-images with different values of λ are displayed. It can be seen that in all cases the sharp edges are preserved, while decreasing λ leads

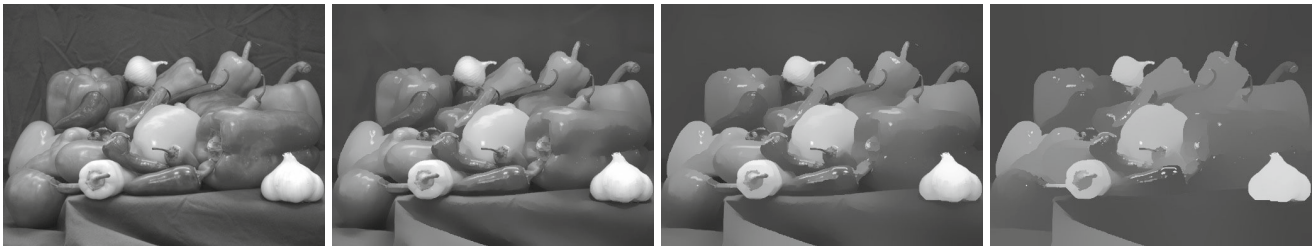

(a) Input image (b) $\lambda = 10^{-4}$ (c) $\lambda = 10^{-6}$ (d) $\lambda = 10^{-8}$

Fig. 3 LS-images for different values of λ (β is fixed at 3000).

(a) Input image (b) 4 neighbors (c) 3×3 neighbors (d) 5×5 neighbors

Fig. 4 The effect of using different neighborhoods $N(i)$ for LS-images; $\beta = 1000$ and $\lambda = 10^{-4}$ are used from (b) to (c).

to smoother images. In experiments, we find that $\lambda = 10^{-4}$ or $\lambda = 10^{-6}$ provides satisfactory results for most images.

Figure 5 shows LS-images with different values of β, which controls the edge-preservation extent. Larger β preserves more sharp edges. If the variance of the grey of color is small, the parameter should also be small. For example, the variance of color in Fig. 9 is small, so choosing a smaller $\beta = 100$ would get desirable result. However, it is difficult to find a fixed or an automatic value for β for all images.

4.3 Comparisons with other methods

In this paper, we have carefully tuned the parameters used for all the methods compared, in order to generate the best results.

Guided filtering. We compare our method with the explicit guided image filtering method [11] in Fig. 6, which demonstrates that our method can preserve weaker edges in the sky region indicated by a box, while guided filtering cannot. As analysed in Ref. [11], smoothing of weaker edges is a limitation of explicit methods such as bilateral filtering and guided filtering. Our LS-image approach, being an implicit method, can preserve weaker edges to some extent at the price of more greater computational cost.

Weighted least-squares method. In Fig. 2, we compare our LS-image with the WLS method [5]. Our results are better than those of WLS, especially within the red box indicated. However, the WLS method is faster than our method. The time taken by WLS and our method is 0.8 s and 2.5 s respectively.

***L_0* gradient minimization.** In Fig. 7, we compare our LS-image with L_0 gradient minimization [9]. Our result can preserve sharp edges better than theirs, as shown in the highlighted box. Meanwhile, our approach takes about 3 s, which is much faster than the L_0 gradient minimization cost of about 78 s for the CUP version.

Local Laplacian filter. Figure 8 compares our LS-image approach with local Laplacian filters via a Laplacian pyramid, as in Ref. [10]. Both methods can preserve sharp edges, but our result is globally brighter and closer to the original image than theirs, especially in the indicated region showing hair and hat. This is because the local Laplacian filters just modify the coefficients of the Laplacian pyramid to obtain the final result without a data term to ensure closeness to the original image.

Other previous work. In Fig. 9, we compare our LS-image result with other classic previous edge-preserving smoothing methods: bilateral filtering [3],

(a) Input image (b) $\beta = 1500$ (c) $\beta = 500$ (d) $\beta = 100$

Fig. 5 LS-images with different values of the parameter β (λ is fixed at 10^{-4}).

(a) Input image (b) Result of guided filtering (c) Our LS-image

Fig. 6 Comparing our method with the guided filtering [11]. (a) Input image; (b) the guided filtering result ($r = 16, \varepsilon = 0.1^2$); and (c) our LS-image ($\beta = 1000, \lambda = 10^{-4}$).

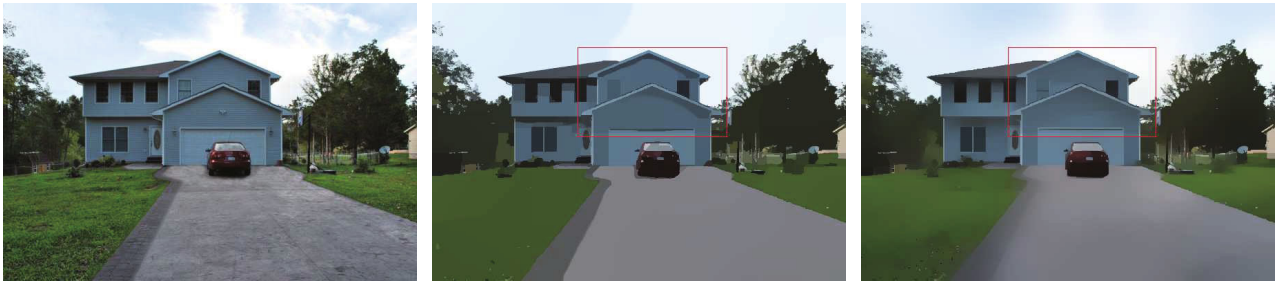

(a) Input image (b) L_0 minimization ($\lambda = 0.0015, \kappa = 1.05$) (c) Our approach ($\beta = 1000, \lambda = 10^{-6}$)

Fig. 7 Comparing LS-images with L_0 gradient minimization ((a) and (b) are directly reproduced from Ref. [9]).

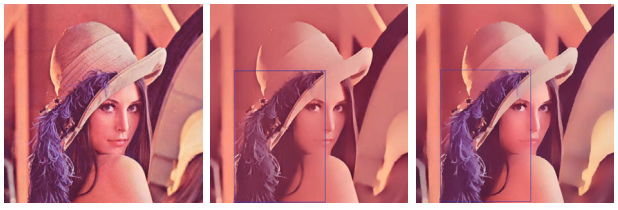

Fig. 8 The Lena image (left) smoothed using local Laplacian filters [10] (middle) and our method with $\beta = 500$ and $\lambda = 10^{-5}$ (right).

the mean-shift method [4], total variation [2], weighted least-squares optimization [5], and L_0 gradient minimization [9, 12]. It can be clearly shown that our method achieves comparable results to L_0 gradient minimization [12] for the step edge image, and generates better results than the other methods.

5 Applications

The proposed LS-image has many potential applications. We apply it to detail manipulation, edge enhancement, and clip-art JPEG artifact removal.

5.1 Detail manipulation

An LS-image $\boldsymbol{u}$ can be seen as a smoothed base layer of the original image $\boldsymbol{g}$ in Eq. (3). Thus the original image can be decomposed as follows:

$$\boldsymbol{g} = \boldsymbol{u} + \boldsymbol{d} \tag{6}$$

where $\boldsymbol{d}$ is the detail. Boosting the detail $\boldsymbol{d}$ can achieve detail manipulation.

Figure 10 shows that boosting using different smoothed layers can produce versatile detail manipulation effects.

5.2 Clip-art compression artifacts removal

Current image compression standards, such as JPEG, when used with low bit rates lead to annoying

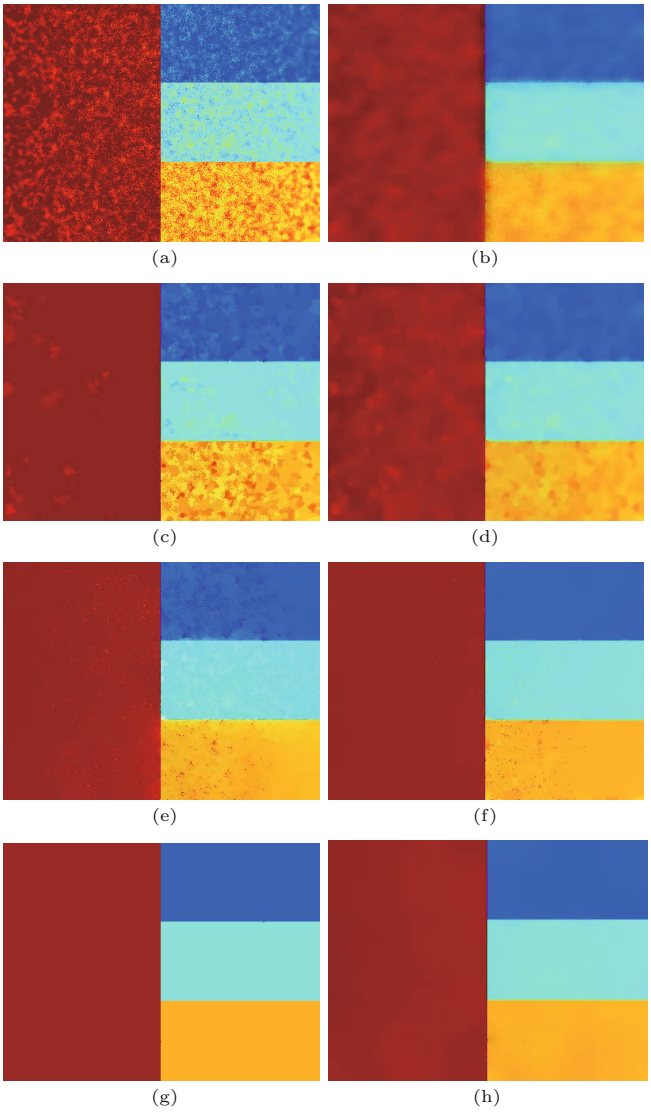

(a) (b) (c) (d) (e) (f) (g) (h)

Fig. 9 (a) Image from Ref. [5], with added noise. Results using: (b) bilateral smoothing [3] ($\delta_s = 12$, $\delta_r = 0.5$); (c) mean-shift smoothing [4] ($h_s = 10$, $h_r = 8$); (d) total variation [2] ($\lambda = 3$); (e) weighted least-squares optimization [5] ($\lambda = 2$, $\alpha = 3$); (f) L_0 gradient minimization [9] ($\lambda = 0.3$, $\kappa = 2$); (g) Cheng et al.'s method [12] ($\lambda = 0.45$); and (h) our method ($\beta = 100$, $\lambda = 10^{-6}$).

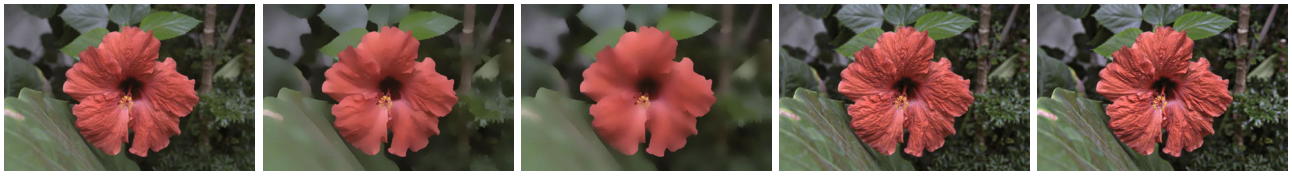

(a) Input image (b) LS-image ($\beta = 1000$) (c) LS-image ($\beta = 200$) (d) Boosted from (b) (e) Boosted from (c)

Fig. 10 Detail manipulation. (a) Input image; (b) and (c) two LS-images with different values of β (λ is fixed to 10^{-5}); (d) and (e) enhanced results boosting detail, based on (b) and (c) respectively (2.0×).

visual artifacts, especially for cartoon images. LS-image processing is suitable for removing these artifacts, due to its edge-preserving property, as the approaches in Refs. [9, 12] (see Fig. 11).

5.3 Edge enhancement

Some images like Fig. 12(a) may contain tiny details making them indistinguishable from sharp edges. The output LS-image displayed in Fig. 12(c), whose gradient map is shown in Fig. 12(f), both removes small textures while preserving the main edges (see Fig. 12(i)). The LS-image approach produces better results than the state-of-the-art work in Ref. [9].

6 Conclusions

In this paper, we define least-squares images (LS-images), which have zero inhomogeneous Laplacian and approximate the original image in a least-squares sense, as a novel edge-preserving image smoothing approach. Comparisons with previous state-of-the-art edge-preserving image smoothing methods demonstrate it achieves high quality results. We have also shown that the LS-image approach can be applied to detail manipulation, edge enhancement, and clip-art JPEG artifact removal. A limitation, however, is that the proposed smoothing method cannot extract main structures from complex textured patterns.

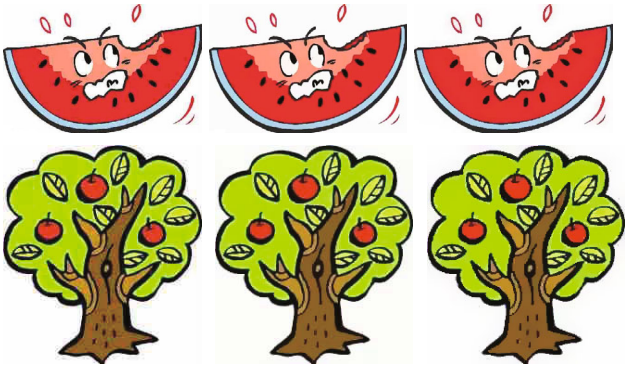

(a) Input images (b) Results in Ref. [9] (c) Our results

Fig. 11 JPEG artifact removal. (a) Low quality JPEG compressed images. (b) Restoration results via L_0 gradient minimization. (c) Restoration via LS-images ($\beta = 1000$, $\lambda = 0.0001$).

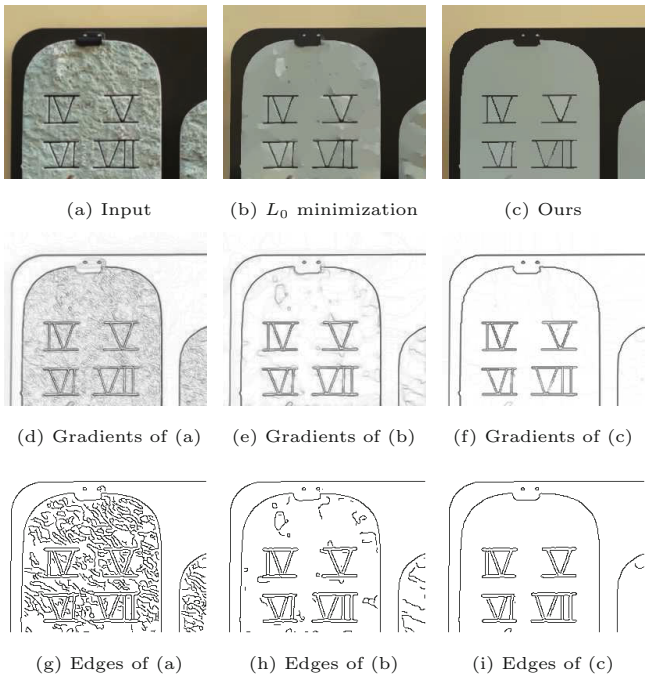

(a) Input (b) L_0 minimization (c) Ours

(d) Gradients of (a) (e) Gradients of (b) (f) Gradients of (c)

(g) Edges of (a) (h) Edges of (b) (i) Edges of (c)

Fig. 12 Smoothing for edge enhancement and detection. Our LS-image (c) ($\beta = 500, \lambda = 10^{-8}$) suppresses low-amplitude details and enhances high contrast edges better than the method in Ref. [9] (b) (figure directly copied from their paper). (d)–(f) are gradient maps of (a)–(c), scaled for visualization. (g)–(i) are Canny edges of (a)–(c).

For future work, we would like investigate further image smoothing methods that minimize other differential quantities, such as curvature. We will also seek further applications for our LS-images, and intend to extend our LS-images to extract structures from complex textures, as in Refs. [22, 25, 27].

Acknowledgements

We would like to thank the anonymous reviewers for their valuable comments. Most images in this paper come from other researchers and we thank them for making their data and code available. The results in Figs. 9(b)–9(g) were shared by the authors of

Ref. [12]. This work is supported by National Natural Science Foundation of China (Nos. 61402300, 61373160, 61363048, 61173102, 61370143, and 61202261), Natural Science Foundation of Hebei Province (No. F2014210127), the Funded Projects for Introduction of Overseas Scholars of Hebei Province, Funds for Excellent Young Scholar of Shijiazhuang Tiedao University, and Scientific and Technological Development Plan of Jilin Province (No. 20130522113JH).

References

[1] Perona, P.; Malik, J. Scale-space and edge detection using anisotropic diffusion. *IEEE Transactions on Pattern Analysis and Machine Intelligence* Vol. 12, No. 7, 629–639, 1990.

[2] Rudin, L. I.; Osher, S.; Fatemi, E. Nonlinear total variation based noise removal algorithms. *Physica D: Nonlinear Phenomena* Vol. 60, Nos. 1–4, 259–268, 1992.

[3] Tomasi, C.; Manduchi, R. Bilateral filtering for gray and color images. In: Sixth International Conference on Computer Vision, 839–846, 1998.

[4] Comaniciu, D.; Meer, P. Mean shift: A robust approach toward feature space analysis. *IEEE Transactions on Pattern Analysis and Machine Intelligence* Vol. 24, No. 5, 603–619, 2002.

[5] Farbman, Z.; Fattal, R.; Lischinski, D.; Szeliski, R. Edge-preserving decompositions for multi-scale tone and detail manipulation. *ACM Transactions on Graphics* Vol. 27, No. 3, Article No. 67, 2008.

[6] Subr, K.; Soler, C.; Durand, F. Edge-preserving multiscale image decomposition based on local extrema. *ACM Transactions on Graphics* Vol. 28, No. 5, Article No. 147, 2009.

[7] Fattal, R. Edge-avoiding wavelets and their applications. *ACM Transactions on Graphics* Vol. 28, No. 3, Article No. 22, 2009.

[8] Farbman, Z.; Fattal, R.; Lischinski, D. Diffusion maps for edge-aware image editing. *ACM Transactions on Graphics* Vol. 29, No. 6, Article No. 145, 2010.

[9] Xu, L.; Lu, C.; Xu, Y.; Jia, J. Image smoothing via L_0 gradient minimization. *ACM Transactions on Graphics* Vol. 30, No. 6, Article No. 174, 2011.

[10] Paris, S.; Hasinoff, S. W.; Kautz, J. Local Laplacian filters: Edge-aware image processing with a Laplacian pyramid. *ACM Transactions on Graphics* Vol. 30, No. 4, Article No. 68, 2011.

[11] He, K.; Sun, J.; Tang, X. Guided image filtering. *IEEE Transactions on Pattern Analysis and Machine Intelligence* Vol. 35, No. 6, 1397–1409, 2013.

[12] Cheng, X.; Zeng, M.; Liu, X. Feature-preserving filtering with L_0 gradient minimization. *Computers & Graphics* Vol. 38, 150–157, 2014.

[13] Levin, A.; Lischinski, D.; Weiss, Y. Colorization using optimization. *ACM Transactions on Graphics* Vol. 23, No. 3, 689–694, 2004.

[14] Grady, L. Random walks for image segmentation. *IEEE Transactions on Pattern Analysis and Machine Intelligence* Vol. 28, No. 11, 1768–1783, 2006.

[15] Sorkine, O.; Cohen-Or, D. Least-squares meshes. In: Proceedings of the Shape Modeling International, 191–199, 2004.

[16] Sorkine, O. Differential representations for mesh processing. *Computer Graphics Forum* Vol. 25, No. 4, 789–807, 2006.

[17] Sorkine, O.; Cohen-Or, D.; Irony, D.; Toledo, S. Geometry-aware bases for shape approximation. *IEEE Transactions on Visualization and Computer Graphics* Vol. 11, No. 2, 171–180, 2005.

[18] Chen, D.; Cohen-Or, D.; Sorkine, O.; Toledo, S. Algebraic analysis of high-pass quantization. *ACM Transactions on Graphics* Vol. 24, No. 4, 1259–1282, 2005.

[19] Chen, J.; Paris, S.; Durand, F. Real-time edge-aware image processing with the bilateral grid. *ACM Transactions on Graphics* Vol. 26, No. 3, Article No. 103, 2007.

[20] Yang, Q.; Tan, K.-H.; Ahuja, N. Real-time O(1) bilateral filtering. In: IEEE Conference on Computer Vision and Pattern Recognition, 557–564, 2009.

[21] Gastal, E. S. L.; Oliveira, M. M. Adaptive manifolds for real-time high-dimensional filtering. *ACM Transactions on Graphics* Vol. 31, No. 4, Article No. 33, 2012.

[22] Cho, H.; Lee, H.; Kang, H.; Lee, S. Bilateral texture filtering. *ACM Transactions on Graphics* Vol. 33, No. 4, Article No. 128, 2014.

[23] Criminisi, A.; Sharp, T.; Rother, C.; Pérez, P. Geodesic image and video editing. *ACM Transactions on Graphics* Vol. 29, No. 5, Article No. 134, 2010.

[24] Gastal, E. S. L.; Oliveiral, M. M. Domain transform for edge-aware image and video processing. *ACM Transactions on Graphics* Vol. 30, No. 4, Article No. 69, 2011.

[25] Karacan, L.; Erdem, E.; Erdem, A. Structure-preserving image smoothing via region covariances. *ACM Transactions on Graphics* Vol. 32, No. 6, Article No. 176, 2013.

[26] Huang, S.-S.; Zhang, G.-X.; Lai, Y.-K.; Kopf, J.; Cohen-Or, D.; Hu, S.-M. Parametric meta-filter modeling from a single example pair. *The Visual Computer* Vol. 30, Nos. 6–8, 673–684, 2014.

[27] Xu, L.; Yan, Q.; Xia, Y.; Jia, J. Structure extraction from texture via relative total variation. *ACM Transactions on Graphics* Vol. 31, No. 6, Article No. 139, 2012.
[28] Li, X.-Y.; Gu, Y.; Hu, S.-M.; Martin, R. R. Mixed-domain edge-aware image manipulation. *IEEE Transactions on Image Processing* Vol. 22, No. 5, 1915–1925, 2013.
[29] Zang, Y.; Huang, H.; Zhang, L. Efficient structure-aware image smoothing by local extrema on space-filling curve. *IEEE Transactions on Visualization and Computer Graphics* Vol. 20, No. 9, 1253–1265, 2014.
[30] Zhang, S.-H.; Li, X.-Y.; Hu, S.-M.; Martin, R. R. Online video stream abstraction and stylization. *IEEE Transactions on Multimedia* Vol. 13, No. 6, 1286–1294, 2011.
[31] Kyprianidis, J. E.; Kang, H. Image and video abstraction by coherence-enhancing filtering. *Computer Graphics Forum* Vol. 30, No. 2, 593–602, 2011.
[32] Botsch, M.; Sorkine, O. On linear variational surface deformation methods. *IEEE Transactions on Visualization and Computer Graphics* Vol. 14, No. 1, 213–230, 2008.

Hui Wang is a lecturer in School of Information Science and Technology at Shijiazhuang Tiedao University, China. He received the Ph.D. degree in computational mathematics at Dalian University of Technology in 2013. His research interests include computer graphics, digital geometry processing, and image processing.

Junjie Cao is a lecturer in School of Mathematical Sciences at Dalian University of Technology, China. He received the Ph.D. degree in computational mathematics from Dalian University of Technology. His research interests include shape modeling, image processing, and machine learning.

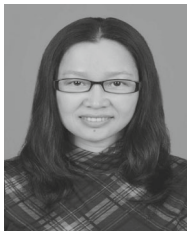

Xiuping Liu is a professor in School of Mathematical Sciences at Dalian University of Technology, China. She received the Ph.D. degree in computational mathematics from Dalian University of Technology. Her research interests include shape modeling and analysis.

Jianmin Wang is an associate professor in School of Information Science and Technology at Shijiazhuang Tiedao University, China. His current research interests include software engineering and network technology.

Tongrang Fan is a professor in School of Information Science and Technology at Shijiazhuang Tiedao University, China. Her current research interests include network technology, network security technology, and intelligent information processing.

Jianping Hu is an associate professor in College of Sciences at Northeast Dianli University, China. He obtained his B.S. and M.S. degrees in mathematics at Jilin University. He received his Ph.D. degree in computational mathematics at Dalian University of Technology in 2009. His research interests include computer graphics, computational geometry, and image processing.